Int. J. Electrochem. Sci., 7 **(2012)** 3089 - 3101

International Journal of
ELECTROCHEMICAL
SCIENCE
www.electrochemsci.org

Electrochemical Monitoring of the Interaction of Cu(II) with Amyloid-*B* Peptides on Boron-Doped Diamond Electrode

Yanli Zhou[1], *Zhaohui Huo*[2], *Xu Zhu*[1], *Xiaohua Zhu*[2], *Maotian Xu*[1,*], *Yong Liang*[2,*]

[1] Henan Key Laboratory Cultivation Base of Nanobiological Analytical Chemistry, Department of Chemistry, Shangqiu Normal University, Shangqiu 476000, People's Republic of China
[2] Department of Chemistry and Environment, South China Normal University, Guangzhou 510631, People's Republic of China
[*]E-mail: xumaotian@sqnc.edu.cn; liangy@scnu.edu.cn

Received: 19 February 2012 / *Accepted:* 12 March 2012 / *Published:* 1 April 2012

Interaction of amyloid-*β* peptides (A*β*), A*β* fragments, and mutated A*β* with Cu(II) was systematically investigated using cyclic voltammetry (CV) on boron-doped diamond electrode with outstanding electrochemical properties. When the same ratio of A*β* to Cu(II) was used, the depressed order of redox current (A*β*(1–42), A*β*(1–16), A*β*(Y–F) > A*β*(H–N) > A*β*(25–35)) was observed for redox activity. Judging by the results of CVs, the resulting mutant A*β*(H–N) showed little affinity with Cu(II) if histidines were mutated individually. The absorption decrease and fluorescence quenching of A*β*(H–N)-Cu(II) were unconspicuous and insensitive compared with that of A*β*(1–16)–Cu(II), further proving that electron structure of tyrosine was not directly attacked and degraded by Cu(II). Almost the same CVs between A*β*(1–16)–Cu(II) and A*β*(Y–F)(tyrosine→phenylalanine)–Cu(II) along with the absence of tyrosine characteristic peak in absorption and fluorescent spectra confirmed that tyrosine was not the potential O ligand. The unchanged redox signal of A*β*(1–16)–Cu(II) compared with A*β*(Y–F)–Cu(II), and the same result of the A*β*(1–42)–Cu(II) and A*β*(25–35)–Cu(II) even the exogenous methionine–Cu(II) clarified that the reduction of Cu(II) was not aroused by Tyr-10 or Met-35 directly.

Keywords: amyloid-*β* peptide; interaction; copper; electrochemistry; boron-doped diamond

1. INTRODUCTION

Alzheimer's disease (AD) is a progressive neurodegenerative disorder and rises almost logarithmically with age. Two major hallmarks of AD are deposition of aggregates of amyloid–*β*

peptides (A*β*) and generation of reactive oxygen species (ROS). First row transition metals including zinc, copper, and iron are highly enriched in A*β* deposition (plaque) of AD [1]. The metal ions are able to bind A*β* directly and modulate aggregation behavior in vitro. For the redox active metal ions like copper and iron are crucial for the production of ROS and oxidative stress [2].

The coordination chemistry between Cu(II) and A*β* has been surveyed by a number of techniques, such as circular dichroism spectroscopy, ultraviolet-visible (UV/vis) spectroscopy, Fourier transform infrared spectroscopy, fluorescence spectroscopy, electron spin resonance, and nuclear magnetic resonance [3–9]. All of the above studies indicate that Cu(II) can be incorporated mainly in the hydrophilic domain (residues 1–16), while contradictory results have been reported regarding the involved ligands and the oxidation state of copper. It has been reported that three imidazole nitrogens from three histidines (His6, His13, His14) and one oxygen-containing group participate in coordination to Cu(II) as the four ligands in a square-planar geometry [10]. So far there remains uncertain regard to the nature of the potential O ligand, though possible candidates include the N–terminal amine, carboxylate groups from aspartic or glutamic acid residues (Asp1 or Glu3) [11, 12], and the sole tyrosine residue (Tyr10) [10,13]. Rat A*β* with Gly5, Phe10, and Arg13, which differs from human A*β* (Arg5, Tyr10, and His13) by three substitutions, does not reduce Cu(II) and Fe (III) and is not readily precipitated by Zn(II) or Cu(II) [14,15]. The results indicate the importance of the three residues. Considering the above listed possible candidates as O ligand, Tyr10 should be provided further exploration.

The "A*β* cascade hypothesis" suggests that A*β* aggregates trigger a complex pathological cascade in AD and lead to neurodegeneration including generation of H_2O_2 [16–19] and free-radical induced oxidation [20–23]. Current research shows inconsistencies in the interpretations of the redox reactions of the A*β*–metal complexes. There are still many aspects that need to be further explored e.g., whether Cu(II) can be reduced by A*β*, and if the reduction does occur which constituents cause the reduction. The hypothesis for Cu(II) reduction as the basis of the oxidative stress appears to be associated with an electron emanating from Tyr10, and the process reduces Cu(II) to Cu(I) and leaves a tyrosyl free radical [24]. However, Zhou's group compared the potentials measured for A*β*–Cu and doubted about participation of Tyr10 in the reduction of A*β*–Cu complexes [25]. Met35 is another controversial residue. The oxidation of the thioether moiety of Met35 to its sulfoxide form in A*β*(1–40) has been proposed to be involved in aggregation, lipid peroxidation, and redox chemistry in association with the metal center [26–28]. However, Silva et al. showed that Met35 did not reduce A*β*–Cu, because A*β*(1–16) which did not contain a Met35 exhibited metal-centered oxidative catalysis [29].

Considering the similarity of biological process and electrochemical reactions, electrochemical methods can allow for the accurate and direct determination of potentials and currents of redox-active biomolecules and provide insight about the electron transfer reactions [30,31]. Thus, electrochemical methods can simulate the redox mechanism of organisms and further get more information compared with other methods. The above mentioned report has studied the electrochemical act of copper

complexes formed with different A*β* fregments and the A*β*–Cu(II) [25]. Brzyska et al. also characterized electrochemical properties of A*β*(1–40)–Cu complexes and demonstrated that the complexation led to conformational changes then reduced the metal electrochemical activity [32]. However, the relevant literatures about current-voltage properties of appointed mutant A*β*–Cu complex have not been traced. In addition, boron-doped diamond (BDD) thin-film is a kind of novel carbon material and is gaining big interest. BDD electrode possess many outstanding properties as described below [33,34]: (i) wide electrochemical potential window in aqueous electrolyte solutions, (ii) low and stable capacitive background current, (iii) high resistance to deactivation by fouling due to low and weak adsorption of polar molecules, (iv) high response reproducibility and long-term response stability, and (v) biocompatibility. Thus, these prominent properties make the BDD thin film an ideal electrode substrate for the study of redox properties of biomolecules, and high sensitivity and facile electron transfer rates is expected to be obtained.

In this work, to probe the amino acid residues in A*β*–Cu(II) involved in binding and reduction, a systematic effort has been made to measure accurately the redox acts of Cu(II) with full-length, different segments and mutant A*β* on BDD electrode, simultaneously assisting absorption and fluorescence spectroscopy. Supported by electrochemical method, further advances in understanding the N coordination of Cu(II) have been provided. The Cu(II)/Tyr hypothesis was tested using an A*β*(Y–F) peptide with Tyr10 substituted with phenylalanine. In terms of the redox mechanism, strong evidence about the inability of Tyr10 and Met35 for reduction Cu(II) was also recorded.

2. EXPERIMENTAL PART

2.1. Materials and Reagents

BDD thin films were prepared by hot–filament chemical vapor deposition on silicon (100) wafers. To enhance nucleation, Si substrates were abraded with 1 μM diamond powder, and then ultra-sonically cleaned successively in acetone and in pure water for 1 min. Ta wires of 0.6 mm in diameter and 14 cm in length were used as filaments. The experimental conditions were: filament-substrate distance: 6 mm, T_{filament}: 2100 ± 200 ºC, $T_{\text{substracte}}$: 850 ~ 950 ºC, vapor pressure: 1.7 KPa, H_2 flow rate: 200 sccm. Acetone was used as carbon source and its concentration (CH_3COCH_3/H_2, V/V) was 3%, while trimethyl borate dissolved in the acetone was used as boron source at a B/C molar ratio of 0.5%.

A*β*(1–16), A*β*(25–35), A*β*(1–42), and mutant A*β* were purchased from the Chinese Peptide Co. (China). To avoid the occurrence of substantial aggregation and to rid the any aggregates of solution, A*β* was dissolved to 2 mg mL^{-1} in 1,1,1,3,3,3-hexafluoroisopropanol (HFIP, Acros, USA), and then incubated overnight at room temperature and stored at −20 °C. HFIP was evaporated off by N_2 gas and the peptide was redissolved in dimethyl sulfoxide (Sigma, USA) to a concentration of 2 mM as stock solution. Throughout the work, 10 mM $Cu(NO_3)_2$ dissolved in 0.2 M KCl was used as the Cu(II) stock

solution. Other chemicals were of analytical grade. The water used was deionized water and obtained from a Millipore M-Q purification system (18 MΩ cm).

Analogues of A*β*(1–16) in which all His residues have been replaced by asparagine or in which Tyr10 residue has been substituted by phenylalanine have been used. Not specified, all the A*β*–Cu complexes were incubated at 37 °C for 90 min in constant temperature incubation box.

Designation Sequence

A*β*(1–16): DAEFRHDSGYEVHHQK
A*β*(H–N) : DAEFRNDSGYEVNNQK
A*β*(Y–F): DAEFRHDSGFEVHHQK
A*β*(25–35): GSNKGAIIGLM
A*β*(1–42): DAEFRHDSGYEVHHQKLVFFAEDVGSNKGAIIGLMVGGVVIA

2.2. Atomic force microscopy (AFM)

An atomic force microscope (Agilent 5500, Agilent Technologies, USA) was used to characterize the morphology of A*β* which was taken out from incubation at certain surroundings (in the presence or absence of Cu(II)). The samples were deposited on mica substrates which firstly were deposited and adsorbed nickel salt for 5 min, then rinsed twice with 200 μL deionized water, and finally dried up with a weak flow of N_2 gas for 1 min. All experimental data were collected in tapping mode in air at optimal force.

2.3. Electrochemical measurements

All electrochemical experiments were conducted on a CHI660D electrochemical workstation. Before use, the BDD electrodes were sonicated successively in 2-propanol and deionized water for 15 min. Glassy carbon (GC) electrodes were polished with 4.0, 1.0 and 0.05 μm alumina powder in succession, rinsed thoroughly with deionized water between each polishing step, and then sonicated in acetone and deionized water in succession. The thin-film electrodes including BDD and GC electrodes were mounted on the bottom of the glass cell by use of a silicone O-ring with an exposed area of 0.07 cm^2. All experiments were performed in a three-electrode cell system with the BDD film or GC as the working electrode, a platinum wire as the auxiliary electrode, and saturated calomel electrode (SCE) as the reference electrode, respectively. 0.2 M KCl solution in deionized water was used as the supporting electrolyte solution (pH 6.9). In cyclic voltammograms (CV) experiments, sweep rate was 0.05 V s^{-1}. To avoid slow precipitation of copper salt, the concentrations of $Cu(NO_3)_2$ solutions were lower than 10^{-4} M. All experiments were carried out at room temperature.

2.4. Absorption spectroscopy measurements

UV/vis absorption measurements were performed in the 200–800 nm range at room temperature with a UV 2300 Spectrophotometer (Spain) in a 1 cm path length quartz cuvette. UV/vis absorption titrations were recorded by adding aliquots of Cu(II) to the cuvette containing a known initial concentration of peptide. No turbidity was observed, indicating the absence of high aggregates of A*β*.

2.5. Fluorescence spectroscopy measurements

Fluorescence measurements of the Tyr residue at position 10 in A*β* were conducted at room temperature using a Cary Eclipse spectrofluorometer (Varian Inc., Palo Alto, CA). An excitation frequency of 280 nm was used and data was collected over the range of 290–400 nm. Samples were placed in a four–sided quartz fluorescence cuvette (Hellma) and data was recorded at room temperature.

3. RESULTS AND DISCUSSION

3.1. AFM research on Aβ aggregate formation

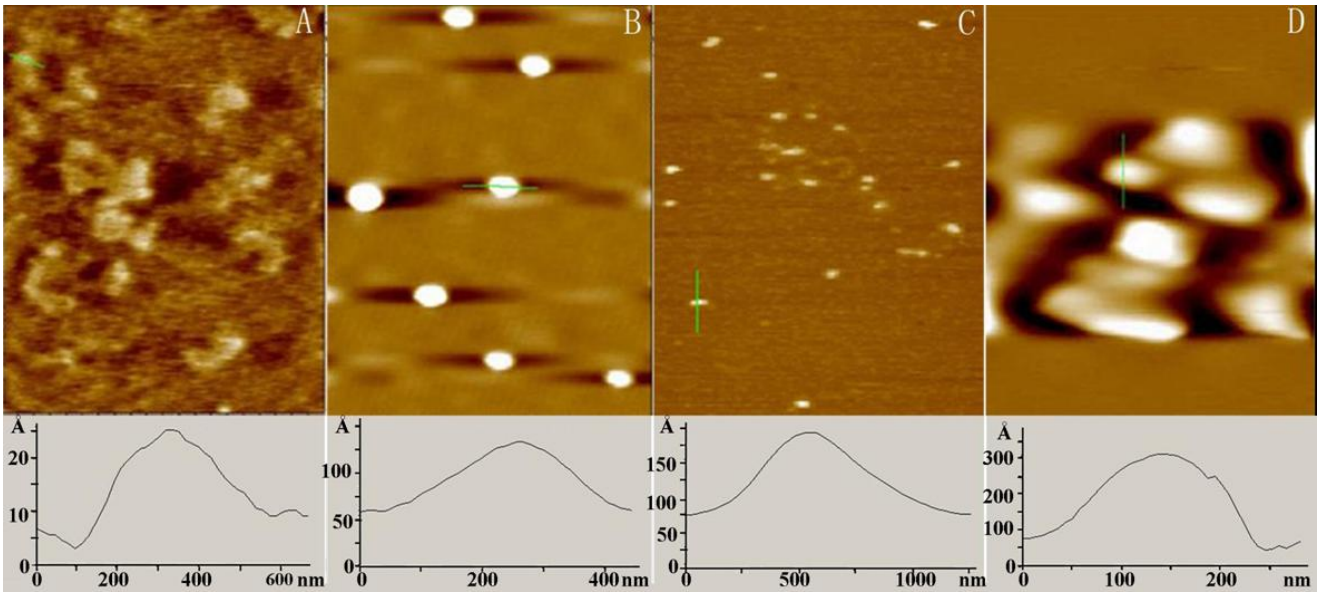

Figure 1. Representative AFM images of A*β* deposits formed on mica substrates in the absence or presence of Cu(II). The deposits were obtained by incubating freshly prepared A*β*(1–16) (5.0 μM) in 0.2 M KCl containing 5% Me_2SO (v/v) (A) without metal ion, (B) with 100.0 μM Cu(II) at 37 °C for 1.5 h. Except that the A*β*(1–16) was replaced with A*β*(1–42), (C) and (D) are the same as (A) and (B), respectively. The size of each AFM image is 4 μm × 4 μm.

The abnormal deposition and aggregation of Aβ on brain tissues are considered to be one of the characteristic neuropathological features of AD. AFM, as an indispensable tool on the field of scientific research of life, is able to capture nm-scale structures adsorbed onto the surface and is commonly used to track the aggregation of Aβ. Fig. 1 shows the investigation of the effect of Cu(II) on the aggregate morphology of Aβ(1–16) and Aβ(1–42). Single and fresh Aβ(1–16) or Aβ(1–42) scarcely aggregated, especially hydrophilic Aβ(1–16) (z-height ~ 2 nm). When Cu(II) was incubated with Aβ(1–16), well-distributed aggregates with fairly standard spherical deposits were observed on the mica substrates (Fig. 1B), with the average z-height ~7 nm recorded. If replaced by Aβ(1–42), in which case voluble and amorphous deposits were found, and the average z-height was threefold against Aβ(1–16)–Cu(II) (Fig. 1D). It was not, however, possible to morphologically distinguish aggregates. The results were in accordance with previous investigations in which aggregates formed in the presence of a molar excess of divalent metal ions and failed to attain classic morphology of amyloid fibrils [35, 36].

3.2. Redox reactions of Aβ–Cu(II) complexes on BDD electrodes

The intrinsic redox properties of Cu(II) are important for a better understanding of the potential redox ligands on A*β* for Cu(II). However, different buffering conditions and electrodes resulted in value of registered reduction potentials of A*β*–Cu(II) complexes differently. In the presence of phosphate buffer solution, which represents a more "physiological" approach towards buffering system, the second step of Cu(I) reduction disappeared and the intensity of Cu(II)/Cu(I) reduction current became small in the presence of A*β*. Hureau et al. found that the electrochemical signature of A*β*–Cu(II) complex in pure water was identical to that in the selective buffer and chloride ions did not strongly affect the CV [37]. Moreover, considering the superior electrochemical properties and inherent biocompatilibility of BDD thin film, CVs in this study were performed on BDD electrodes using 0.2 M KCl as supporting electrolyte solution.

The electrochemical behaviors of 100.0 μM Cu(II) at BDD and GC electrodes were studied by CVs (Fig. 2). At the GC electrode, there was a broad reduction peak with great background absorption, standing in marked contrast with BDD electrode at which significant improvement of the peak current together with the sharpness of the peak and low background current was observed due to its outstanding electrochemical properties. The above results demonstrated that BDD thin-film as an efficient promoter enhanced the kinetics of the electrochemical process, and was expected to obtain the sensitive detection in the interaction of biomolecules and metal ions.

Due to the metal coordination spheres, conformational consequences and relative binding affinities of peptides for Cu(II), the redox current and potential of the resultant copper complexes varied. Voltammetry is a convenient method to monitor subtle changes in the redox properties of electroactive species and reflect the interactions.

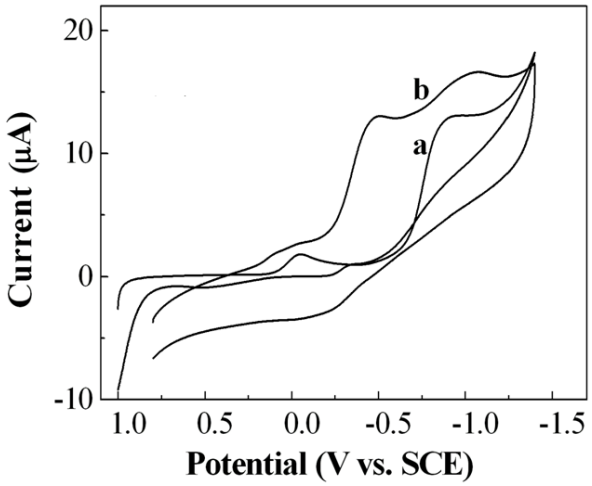

Figure 2. CVs of 100.0 μM Cu(II) in 0.2 M KCl at the BDD electrode (a) and GC electrode (b).

In Fig. 3, CVs of Cu(II) without A*β*, with A*β*(1–16), A*β*(1–42), and A*β*(25–35) are shown as black, red, blue and magenta curves, respectively. As for A*β*(1–16) and A*β*(1–42), the peak at ~ –0.25 V were assigned to the reduction of A*β*–Cu(II) to A*β*–Cu(I) and ~ –0.89 V to the reduction of A*β*–Cu(I) to A*β*–Cu(0). The comparison of the voltammograms of A*β*(1–16)–Cu(II) or A*β*(1–42)–Cu(II) with free Cu(II) showed that the reduction current of the complex was smaller, even though the concentration of the former was equal to that of the latter. This suggested that Cu(II) was in complex form, and coefficient conformational changes diminished copper accessibility to the external environment. In other words, the A*β*(1–16)–Cu(II) or A*β*(1–42)–Cu(II) had a smaller diffusion compared with pure Cu(II).

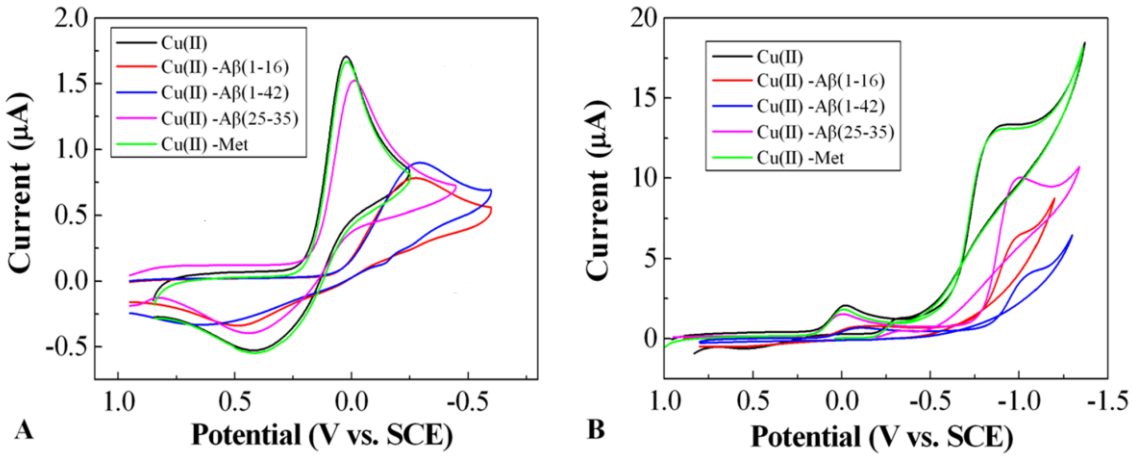

Figure 3. CVs (A and B) of 100.0 μM Cu(II) in 0.2 M KCl containing 5% Me_2SO (v/v) without A*β* (black), with 10.0 μM A*β*(1–16) (red), A*β*(1–42) (blue), A*β*(25–35) (magenta), and Met (green).

In the cathodic range, the redox behavior of the A*β*(1–42)–Cu was highly comparable to that of A*β*(1–16) counterpart (Fig. 3). As we know, A*β*(1–42) was prone to aggregation and caused a significant adsorption onto the electrode surface. Thus, our results also proved that BDD electrodes had perfect anti-adsorption ability to alleviate this effect and could provide the stable results. Compared with the obvious potential shifts and intensity changes in the presence of A*β*(1–16) or A*β*(1–42), there was scarcely any changes for Cu(II) when adding A*β*(25–35) (Fig. 3). The addition of external Met to Cu(II) did not create a current increase at –0.89 V which signified the transition Cu(I)–Cu(0). Similarly there was lack of direct electrochemistry evidence for the change of oxidation state of Cu(II) in A*β*(25–35) even in Met. E_{Met} (0.71 V) was higher than $E_{A\beta(1-40)-Cu(II)}$, which gave a dramatic 68.5 kJ difference in Gibbs free energy or a negligibly small equilibrium constant (9.8×10^{-13}) for one-electron reduction of A*β*(1–40)–Cu(II) by Met at 298 K [38]. The result demonstrated that Met, internal or external, was not needed for the metal-centered oxidation reaction.

There are four residues including three His residues (His6, His13, and His14) and one Tyr residue (Tyr10) in A*β*(1–42) that are known as the possible binding sites of the A*β*–Cu complex. Structural and metal-binding studies had proved that mutations substantially altered the coordination and metal-binding properties of the proteins [39,40].

To identify the binding sites, A*β*(1–16) and site-directed mutant A*β*(1–16) (A*β*(Y–F) and A*β*(H–N)) have been selected. When the same ratio A*β* to copper was used, the rank order of inhibitory effect (A*β*(1–42) ≈ A*β*(1–16) ≈ A*β*(Y–F) > A*β*(H–N)) was observed for redox activity (Fig. 4). Marked difference in the redox activity was observed for Cu(II) with A*β* segments including or excluding His. When Cu(II) affected with A*β*(1–42), A*β*(1–16) and A*β*(Y–F) that contained His residues, it expressed fierce peak current diminution, while redox behavior of A*β*(H–N)–Cu(II) which was exclusive His residues tended to analogous to pure Cu(II).

The result indicated that three His residues were assigned to the binding sites. Similar change did not discover for A*β* whether contain Tyr, eliminating Tyr10 as the potential O ligand. In addition, for A*β*(Y–F)–Cu(II) and A*β*(1–16)–Cu(II), the almost equal current intensity at –0.89 V excluded the possibility that Cu(II) center can be reduced by Tyr10. To reduce Cu(II), a species must have a reduction potential that is more negative than 0.02 V (vs. SCE) in our system, while oxidation potential of Tyr10 is ~0.78 V [25].

Cu(II) and Zn(II) share common binding sites, and Zn(II) is also displaced from A*β* when it is co-incubated with excess Cu(II) [41,42]. To illustrate the effect of Zn(II) on the complexes of the A*β*–Cu, Fig. 5 reveals CVs of A*β*(1–16) incubated with Cu(II) (curve a), with both Cu(II) and Zn(II) for 90 min (curve b), and firstly with Zn(II) for 5 h then with Cu(II) for 90 min(curve c). We should note that, with background subtraction, there was little change compared with A*β*(1–16)–Cu(II) prior to the addition of Zn(II), demonstrating that Zn(II) with weaker binding affinity (K_d of high-affinity Zn(II) binding was about 100 nM, and for low-affinity binding was about 5 μM) could not compete with Cu(II) ($K_d \approx 5.0 \times 10^{-11}$ M) [43].

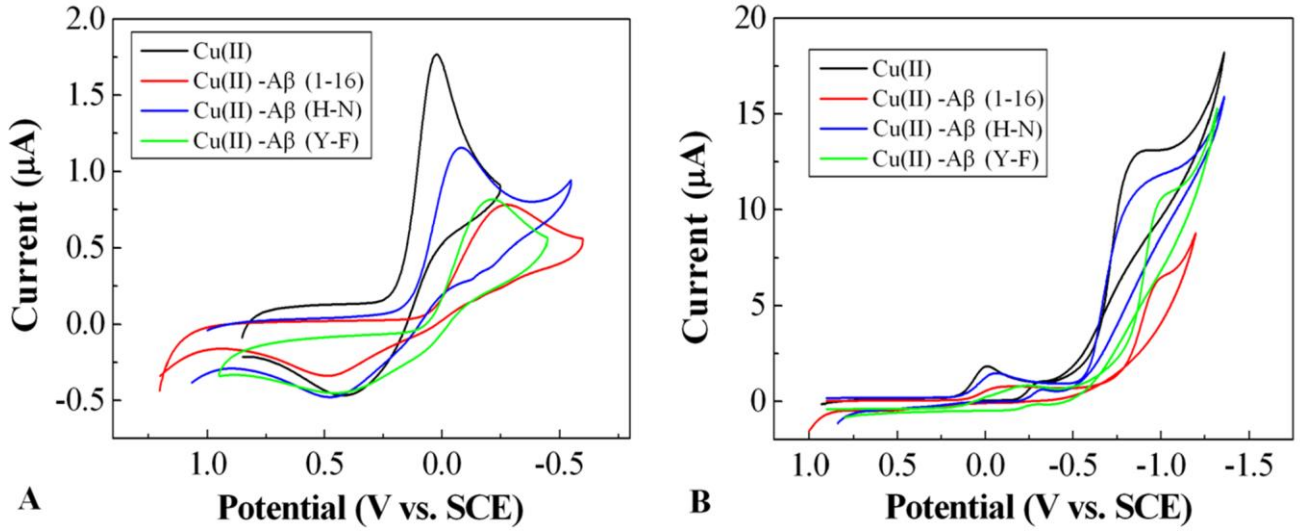

Figure 4. CVs (A and B) of 100.0 μM Cu(II) in 0.2 M KCl containing 5% Me_2SO (v/v) without A*β* (black), with 10.0 μM A*β*(1–16) (red), A*β*(H–N) (blue), and A*β*(Y–F) (green).

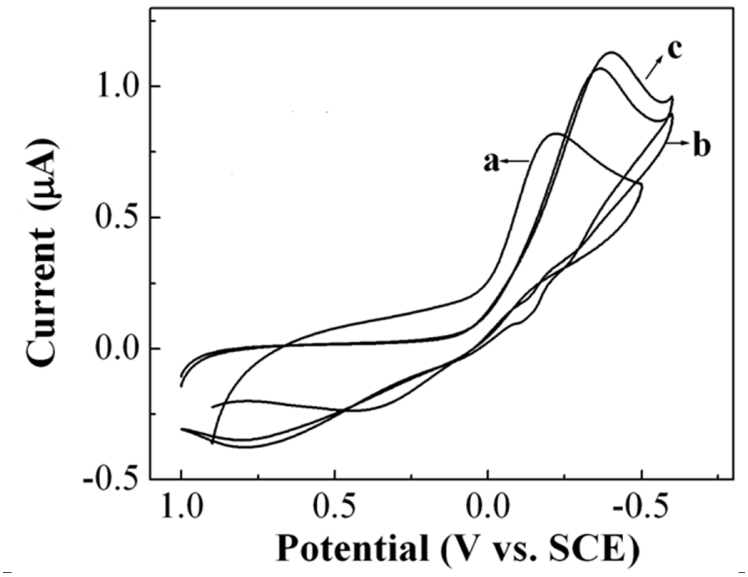

Figure 5. CVs of 10.0 μM A*β*(1–16) incubated with 100.0 μM Cu(II) for 90 min (**a**), with both 100.0 μM Cu(II) and 100.0 μM Zn(II) for 90 min (**b**), and with firstly 100.0 μM Zn(II) for 5 h and then with 100.0 μM Cu(II) for 90 min (**c**) in 0.2 M KCl containing 5% Me_2SO (v/v).

3.3. Absorption Spectroscopy

UV/vis absorption measurement is a very simple method and is applicable to explore the structural change and to know the complex formation [44]. Aromatic group of Tyr10 contains mobile π

electrons which correspond to the π→π* transition. Hence, absorption spectrum of natural A*β*(1–16) and mutant Aβ(H–N) in presence and absence of Cu(II) were recorded (Fig. 6). Upon addition of 200.0 μM Cu(II), the A*β*(1–16) absorption intensity at ~275 nm for aromatic group of Tyr10 decreased and substantially vanished in Fig. 6A. The absorption spectroscopy in the range of 390–460 nm showed no absorption bands, indicating the binding of Cu(II) with Tyr [45,46]. Merely an increase in the absorbance of A*β*(1–16) at ~265 nm was observed upon Cu(II) binding, together with the small broad absorption in the range of 290~340 nm. These changes could be attributed to ligand-to-metal charge transfer (LMCT) processes, viz., from His to the Cu(II). However, as shown in Fig. 6B, in contrast with natural A*β*(1–16) the absorption peak (275 nm) of A*β*(H–N) decreased unconspicuously with the increasing concentration of Cu(II), demonstrating that π→π* transition of Tyr10 in A*β*(H–N) was not directly attacked and degraded by Cu(II). There was little conformational changes for A*β*(H–N) by adding Cu(II). The result was agreement with the above electrochemical conclusion that His had the strongest metal binding affinities.

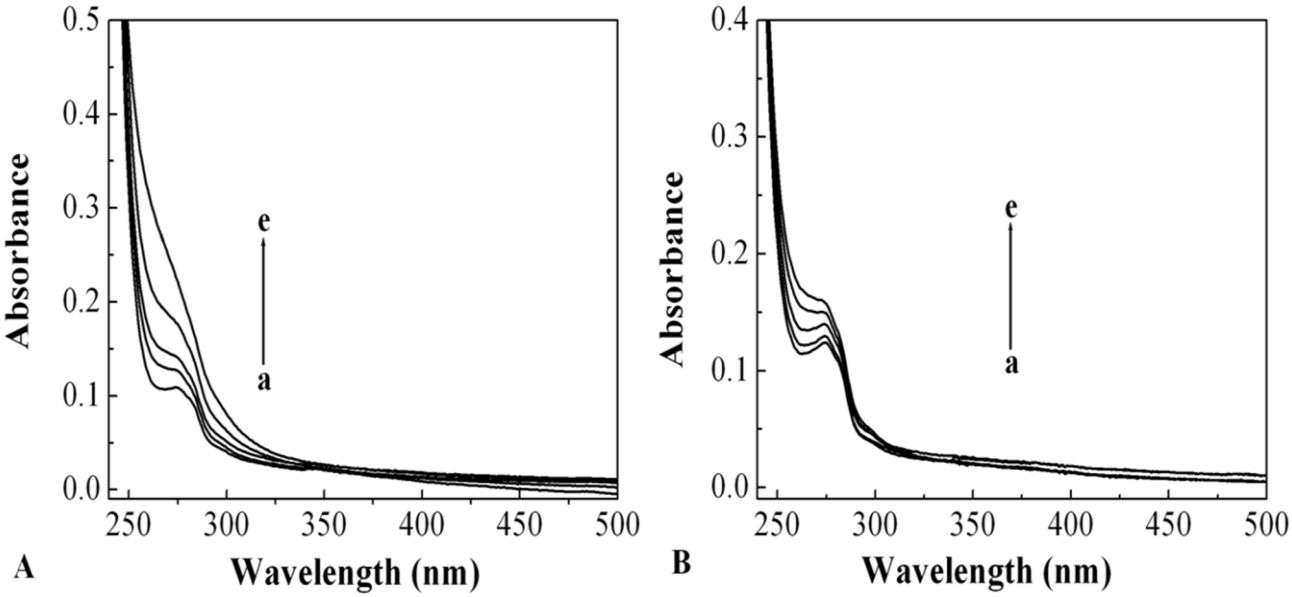

Figure 6. Intensity of absorption spectra for A*β*(1–16) (A) and A*β*(H–N) (B) after addition of Cu(II) in 0.2 M KCl containing 5% Me_2SO (v/v). *c*(A*β*(1–16)) = 50.0 μM, *c*(A*β*(H–N)) = 50.0 μM, (a–e) *c*(Cu(II)): 0, 50.0, 100.0, 150.0 and 200.0 μM.

3.4. Fluorescence Spectroscopy

Based on the fluorescene signal of Tyr, the fluorescence spectra (excitation at 280 nm) of 50.0 μM natural A*β*(1–16) or mutant A*β*(H–N) were obtained in the presence of varied concentrations of Cu(II), as shown in Fig. 7A. Upon addition of Cu(II), the A*β*(1–16) fluorescence intensity decreased and substantially attenuated at a Cu(II)/A*β*(1–16) molar ratio of greater than 2:1.

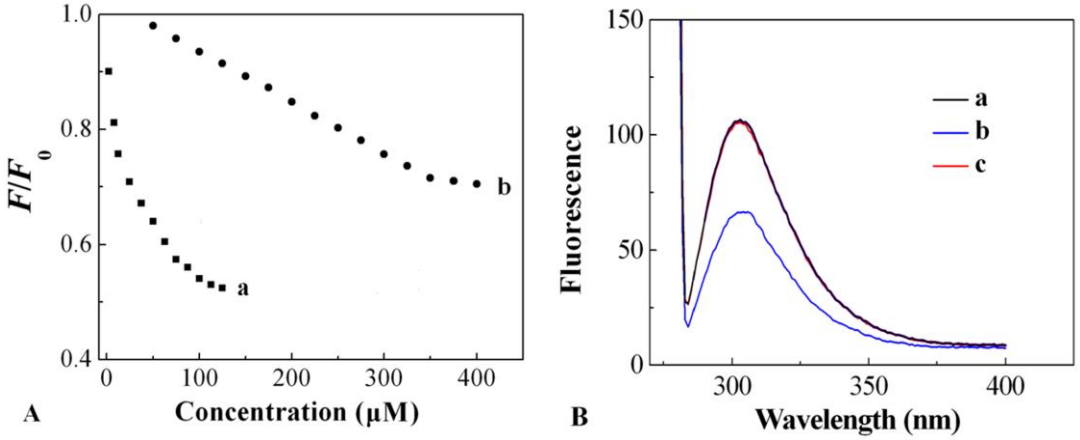

Figure 7. (A) Intensity of fluorescence spectra for 50.0 μM A*β*(1–16) (a) and A*β*(H–N) (b) after addition of Cu(II) in 0.2 M KCl containing 5% Me_2SO (v/v), *c*(Cu(II)) for curve a: 0, 2.5, 8.0, 12.5, 25.0, 37.5, 50.0, 62.5, 75.0, 87.5, 100.0, 112.5 and 125.0 μM, *c*(Cu(II)) for curve b: 0, 50.0, 75.0, 100.0, 125.0, 150.0, 175.0, 200.0, 225.0, 250.0, 275.0. 300.0, 325.0, 350.0, 375.0 and 400.0 μM, F_0 and F are the fluorescence intensities before and after the addition of Cu(II), respectively. (B) Fluorescence spectra of 50.0 μM A*β*(1–16) in 0.2 M KCl containing 5% Me_2SO (v/v) without metal ions (a), with 20.0 μM Cu(II) (b), and with 500 μM Zn(II) (c).

This considerable fluorescence quenching in the presence of micromolar Cu(II) indicated metal complex formation [47]. The influence of His was determined from the plot of fluorescence intensity of A*β*(H–N) versus the Cu(II) concentration. While mutant exhibited minimal quenching until more than 1 equiv of Cu(II) had been added (≈ 25% fluorescence decrease at 6 equiv of Cu(II)). The results also testified that the removal of three His residues reduced the affinity of Cu(II) for A*β*(1–16), which provided sufficient proofs for His as possible ligands.

To further examine Cu(II)/Tyr hypothesis, fluorescence spectra of A*β*(1–16) before and after the addition of Zn(II), with a d^{10} electronic configuration, were investigated in Fig. 7B. There was little quenching even when 10 equiv of Zn(II) had been added, indicating little capacity for flurescence quenching and incapable participation in LMCT. To conclude, Tyr10, which merely remained very close to Cu(II) bound to A*β*, acted as charge donation instead of a tightly bound ligand in A*β*–Cu(II) complexes.

4. CONCLUSIONS

The mechanisms of A*β*–Cu(II) complexes involving the amino acid residues in A*β* for metal binding and reduction were systematically investigated mainly by the electrochemical method on BDD electrodes. By means of AFM, the presence of Cu(II) disabled the fibril formation regarding to the A*β* and its segment. The study of CV and spectroscopy on the complexes of A*β*(1–16), A*β*(1–42), A*β*(25–

35) or mutant Aβ with Cu(II) provided direct evidence that His residues were the most critical ligands for natural copper-binding and the copper binding ability of Aβ was abolished to a great extent without them. However, Tyr10 merely acted as charge donation but not directly involved in binding and reducing the copper center. The analogical intensity of $I_{p(Cu(I)-Cu(0))}$ in Aβ(1–42)–Cu(II), Aβ(25–35)–Cu(II) even the exogenous Met with Cu(II) got rid of Met as reductant. Given the slow and gradual development of AD, our contention appears to be valuable. The experimental results also exhibited that BDD thin film with outstanding electrochemical properties and inherent biocompatilibility was superior electrode material to study the electrochemistry of biomolecules. In the future work, deeply understanding the biochemistry of the metal-Aβ interactions and its relationship with the pathological events of AD still need to be accelerated.

ACKNOWLEDGEMENTS
The authors greatly appreciate the supports of the National Natural Science Foundation of China (Nos. 21105062 and 21175091).

References

1. P. Faller, *ChemBioChem*, 10 (2009) 2837.
2. Y. H. Hung, A. I. Bush and R. A. Cherny, *J. Biol. Inorg. Chem.*, 15 (2010) 61.
3. C. D. Syme, R. C. Nadal, S. E. J. Rigby and J. H. Viles, *J. Biol. Chem.*, 279 (2004) 18169.
4. H. A. Feaga, R. C. Maduka, M. N. Foster and V. A. Szalai, *Inorg. Chem.*, 50 (2011) 1614.
5. M. Nakamura, N. Shishido, A. Nunomura, M. A. Smith, G. Perry, Y. Hayashi, K. Nakayama and T. Hayashi, *Biochemistry*, 46 (2007) 12737.
6. Y. E. Khoury, P. Dorlet, P. Faller and P. Hellwig, *J. Phys. Chem. B*, 115 (2011) 14812.
7. L. Guilloreau, L. Damian, Y. Coppel, H. Mazarguil, M. Winterhalter and P. Faller, *J. Biol. Inorg. Chem.*, 11 (2006) 1024.
8. J. W. Karr, L. J. Kaupp and V. A. Szalai, *J. Am. Chem. Soc.*, 126 (2004) 13534.
9. L. Hou and M. G. Zagorski, *J. Am. Chem. Soc.*, 128 (2006) 9260.
10. A. Jancsó, K. Selmeczi, P. Gizzi, N. V. Nagy, T. Gajda and B. Henry, *J. Inorg. Biochem.*, 105 (2011) 92.
11. J. W. Karr, H. Akintoye, L. J. Kaupp and V. A. Szalai, *Biochemistry*, 44 (2005) 5478.
12. T. Kowalik-Jankowska, M. Ruta, K. Wiśniewska and L. Lankiewicz, *J. Inorg. Biochem.*, 95 (2003) 270.
13. T. Miura, K. Suzuki, N. Kohata and H. Takeuchi, *Biochemistry*, 39 (2000) 7024.
14. B. D. Shivers, C. Hilbich, G. Multhaup, M. Salbaum, K. Beyreuther and P. H. Seeburg, *EMBO J.*, 7 (1988) 1365.
15. C. S. Atwood, R. D. Moir, X. Huang, R. C. Scarpa, N. M. E. Bacarra, D. M. Romano, M. A. Hartshorn, R. E. Tanzi and A. I. Bush, *J. Biol. Chem.*, 273 (1998) 12817.
16. A. Rauk, *Chem. Soc. Rev.*, 38 (2009) 2698.
17. C. Behl, J. B. Davis, R. Lesley and D. Schubert, *Cell*, 77 (1994) 817.
18. L. Guilloreau, S. Combalbert, A. Sournia-Saquet, H. Mazarguil and P. Faller, *ChemBioChem*, 8 (2007) 1317.
19. C. Opazo, X. Huang, R. A. Cherny, R. D. Moir, A. E. Roher, A. R. White, R. Cappai, C. L.

Masters, R. E. Tanzi, N. C. Inestrosa and A. I. Bush, *J. Biol. Chem.*, 277 (2002) 40302.
20. D. A. Butterfield, *Curr. Med. Chem.*, 10 (2003) 2651.
21. H. Engelberg, *Demen. Geriat. Cogn. Disord.*, 18 (2004) 278.
22. A. Granzotto, M. Suwalsky and P. Zatta, *J. Inorg. Biochem.*, 105 (2011) 1066.
23. T. Hayashi, N. Shishido, K. Nakayama, A. Nunomura, M. A. Smith, G. Perry and M. Nakamura, *Free Rad. Biol. Med.*, 43 (2007) 1552.
24. A. I. Bush, *Trends Neurosci.*, 26 (2003) 207.
25. D. Jiang, L. Men, J. Wang, Y. Zhang, S. Chickenyen, Y. Wang and F. Zhou, *Biochemistry*, 46 (2007) 9270.
26. F. E. Ali, F. Separovic, C. J. Barrow, R. A. Cherny, F. Fraser, A. I. Bush, C. L. Masters and K. J. Barnham, *J. Pepetide Sci.*, 11 (2005) 353.
27. D. A. Butterfield and A. I. Bush, *Neurobiol. Aging*, 25 (2004) 563.
28. M. E. Clementi, G. E. Martorana, M. Pezzotti, B. Giardina and F. Misiti, *Int. J. Biochem. Cell Biol.*, 36 (2004) 2066.
29. G. F. Z. Silva, V. Lykourinou, A. Angerhofer and L. J. Ming, *Biochim. Biophys. Acta*, 1792 (2009) 49.
30. A. W. Bott, *Curr. Sep.*, 18 (1999) 9.
31. Y. Peng, C. Wang, H. H. Xu, Y. N. Liu and F. Zhou, *J. Inorg. Biochem.*, 104 (2010) 365.
32. M. Brzyska, K. Trzesniewska, A. Wieckowska, A. Szczepankiewicz and D. Elbaum, *ChemBioChem*, 10 (2009) 1045.
33. A. Kraft, *Int. J. Electrochem. Sci.*, 2 (2007) 355.
34. Y. L. Zhou, J. F. Zhi, Y. S. Zou, W. J. Zhang and S.-T. Lee, *Anal. Chem.*, 80 (2008) 4141.
35. D. P. Smith, G. D. Ciccotosto, D. J. Tew, M. T. Fodero–Tavoletti, T. Johanssen, C. L. Masters, K. J. Barnham and R. Cappai, *Biochemistry*, 46 (2007) 2881.
36. C. Ha, J. Ryu and C. B. Park, *Biochemistry*, 46 (2007) 6118.
37. C. Hureau, V. Balland, Y. Coppel, P. L. Solari, E. Fonda and P. Faller, *J. Biol. Inorg. Chem.*, 14 (2009) 995.
38. C. Schöneich, *Biochim. Biophys. Acta*, 1703 (2005) 111.
39. H. Nicholson, B. F. Anderson, T. Bland, S. C. Shewry, J. W. Tweedie and E. N. Baker, *Biochemistry*, 36 (1997) 341.
40. Q. Y. He, A. B. Mason, R. C. Woodworth, B. M. Tam, T. Wadsworth and R. T. A. MacGillivray, *Biochemistry*, 36 (1997) 5522.
41. D. S. Yang, J. McLaurin, K. Qin, D. Westaway and P. E. Fraser, *Eur. J. Biochem.*, 267 (2000) 6692.
42. A. I. Bush, *Neurobiol. Aging*, 23 (2002) 1031.
43. S. Y. Bi, D. Q. Song, L. Ding, Y. Tian, X. Zhou, Z. Y. Liu and H. Q. Zhang, *Spectrochim. Acta Part A*, 61 (2005) 629.
44. J. A. Halfen, B. A. Jazdzewski, S. Mahapatra, L. M. Berreau, E. C. Wilkinson, L. Que, Jr and W. B. Tolman, *J. Am. Chem. Soc.*, 119 (1997) 8217.
45. M. Vaidyanathan and M. Palaniandavar, *Proc. Indian Acad. Sci.*, 112 (2000) 223.
46. Q. F. Ma, J. Hu, W. H. Wu, H. D. Liu, J. T. Du, Y. Fu, Y. W. Wu, P. Lei, Y. F. Zhao and Y. M. Li, *Biopolymers*, 83 (2006) 20.
47. W. Garzon–Rodriguez, A. K. Yatsimirsky and C. G. Glabe, *Bioorg. Med. Chem. Lett.*, 9 (1999) 2243.